Electronic Supplementary Material (ESI) for Nanoscale.

Supporting Information

Rational Design and Facile Fabrication of Biocompatible Triple Responsive Dendrimeric Nanocages for Targeted Drug Delivery

Dan Zhong,[a] Huayu Wu,[a] Yahui Wu,[a] Yunkun Li,[a] Xianghui Xu,*[ab] Jun Yang,[c] and Zhongwei Gu*[ab]

[a] National Engineering Research Center for Biomaterials, Sichuan University, Chengdu, Sichuan, 610064, P.R. China. E-mail: zwgu1006@hotmail.com; xianghui.xu@hotmail.com

[b] College of Materials Science and Engineering, Nanjing Tech University, Nanjing, Jiangsu, 210009, P.R. China

[c] The Key Laboratory of Bioactive Materials, Ministry of Education, College of Life Science, Nankai University, Tianjin 300071, P.R. China

1. Experimental Section

1.1 Materials

(3-aminopropyl)trimethoxysilane was purchased from Alfa Aesar (Ward Hill, MA). 1-ethyl-3-[3-(dimethylamino)propyl]carbodiimide hydrochlide (EDC·HCl), 2-(1*H*-Benzotriazol-1-yl)-1,1,3,3-tetramethyluroniumhexafluorophosphate (HBTU), 1-hydroxybenzotriazole hydrate (HOBT) and Boc-Lys(Boc)-OH were obtained from GL Biochem (Shanghai, China). *N*,*N*-diisopropylethylamine (DIPEA) and trifluoroacetic acid (TFA) were obtained from Asta Tech Pharmaceutical (Chengdu, China). Methoxypolyethylene glycol (mPEG, Mw = 1000) and lipoic acid (LA) were purchased from Aladdin (Shanghai, China). Dithiothreitol (DTT), glutathione (GSH), pyrene, Nile red, 1,1'-dioctadecyl-3,3,3',3'-tetramethylindocarbocyanine (DiI), 3,3'-dioctadecyloxacarbocyanine perchlorate (DiO), buthionine sulfoximine (BSO), and glutathione monoester (GSH-OEt) were obtained from Sigma-Aldrich Co. (St Louis, USA). Doxorubicin hydrochloride (DOX·HCl) was purchased from Zhejiang Hisun Pharmaceutical Co. (Zhejiang, China). Blab/c mice were purchased from Chengdu Dashuo Experimental Animal Company (Chengdu, China). All the organic solvents were used as received.

1.2 Synthesis of Lipoic Acid Modified Generation 2 Dendrimer (G2-LA_{32})

1.2.1 Synthesis of OAS·HCl

(3-aminopropyl)trimethoxysilane (15 mL, 60 mmol) was slowly added into the mixed solution of methanol (350 mL) and concentrated HCl (30 mL). The solution was stirred at 90 ºC for 24 h. White crude product was obtained by adding 250 mL of tetrahydrofuran (THF) after the solution cooled down to room temperature. Pure product was obtained by washing with THF again and drying under vacuum.

1.2.2 Synthesis of Generation 1 Dendrimers

OAS·HCl (2.5 g, 2.1 mmol), Boc-Lys(Boc)-OH (7.1 g, 21 mmol), HBTU (8.0 g, 21 mmol) and HOBT (2.8 g, 21 mmol) were dissolved in 30 mL of anhydrous DMF under nitrogen atmosphere. The solution was stirred at 0 ºC for 30 min. DIPEA (6 mL,

34 mmol) was added. The reaction mixture was stirred at room temperature for 48 h. After removal of DMF, the residue was dissolved in $CHCl_3$ and washed with saturated $NaHCO_3$, $NaHSO_4$ and NaCl solution for several times. The organic phase was dried with $MgSO_4$ overnight. After removal of $CHCl_3$, the crude product was recrystallized in acetonitrile, then white pure solid product was obtained.

1.2.3 Synthesis of Generation 2 Dendrimers

Generation 1 (2.0 g, 0.6 mmol) in distilled CH_2Cl_2 (5 mL) was treated with TFA (7.4 g, 96 mmol) under nitrogen atmosphere. After stirred for 6 h, the solution was concentrated and anhydrous diethyl ether was added and colorless solid was obtained. Generation 2 dendrimer and lipoic acid modified Generation 2 dendrimer were obtained by repeating the synthesis step of Generation 1.

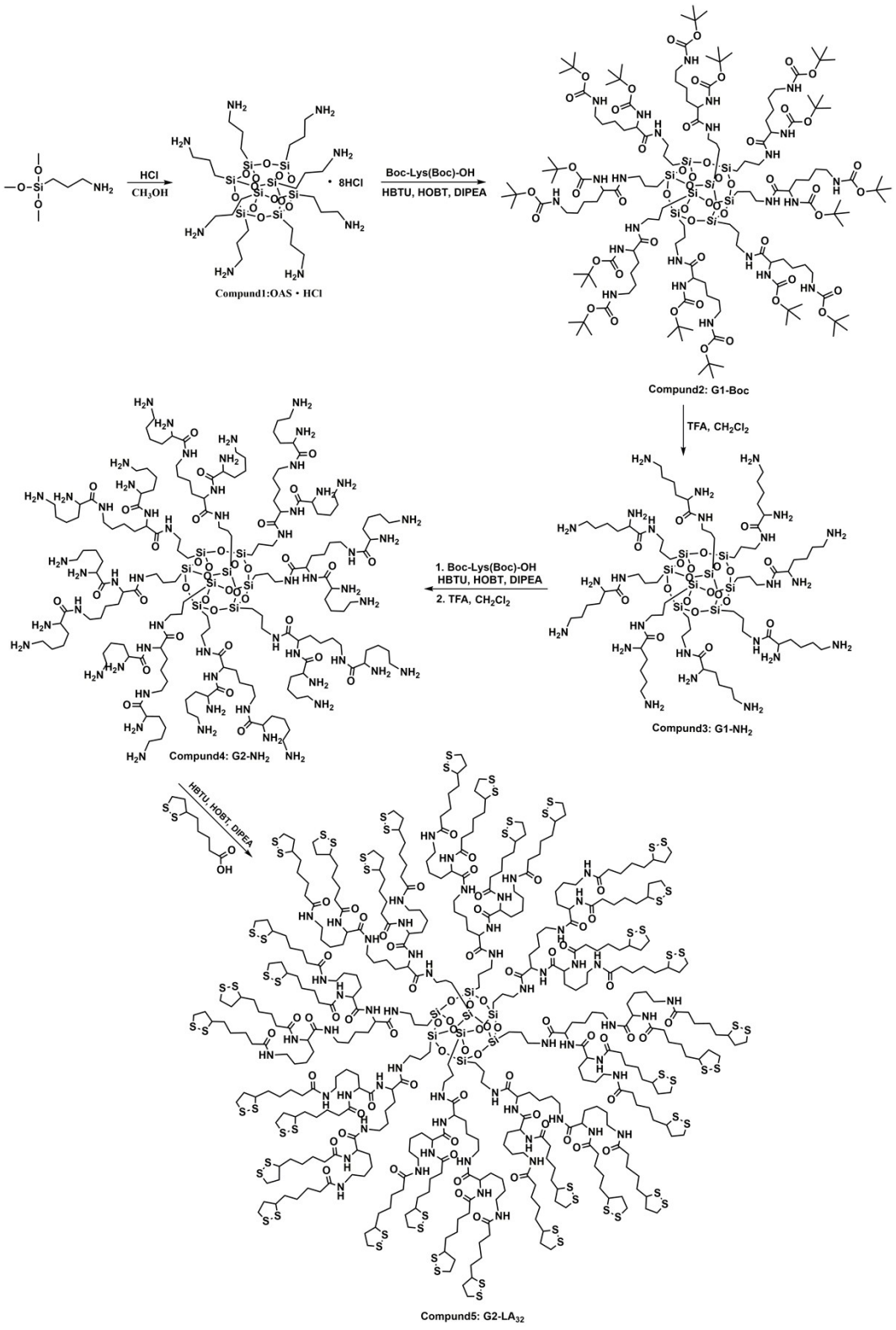

Scheme S1. Synthetic route of lipoic acid modified generation 2 dendrimer.

1.3 Synthesis of mPEG-LA

mPEG (5.0 g, Mw = 1000), lipoic acid (1.6 g, 7.5 mmol), EDC·HCl (1.9 g, 10 mmol) and HOBT (1.4 g, 10 mmol) were dissolved in 50 mL of distilled CH_2Cl_2 under nitrogen atmosphere. The solution was stirred at 0 ºC for 30 min. DIPEA (4.2 mL, 25 mmol) was added dropwise. After reaction at room temperature for 24 h, the mixture solution was washed with saturated $NaHCO_3$, $NaHSO_4$ and NaCl solution for several times. The organic phase was dried with anhydrous $MgSO_4$ for 1 day. After removal of CH_2Cl_2, the residue was purified by silica gel column chromatography using petroleum ether: ethyl acetate (v:v = 1:1) and CH_2Cl_2: CH_3OH (v:v = 50:1) as eluent. Yellow solid was obtained.

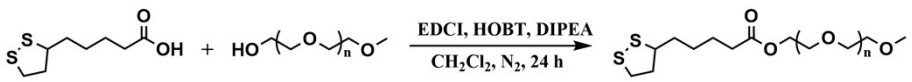

Scheme S2. Synthetic route of mPEG-LA.

1.4 Self-assembly and Critical Aggregation Concentration (CMC)

Pyrene was used as a fluorescent probe to determine the CMC. Briefly, the concentration of pyrene was fixed at 0.6 μM. The concentrations of TDNs and dendrimer assemblies (DAs) were varied from 0.001 to 1 mg/mL. The emission wavelength was set at 395 nm. And the excitation fluorescence at 334 and 338 nm were monitored. The CMC was estimated according to the intersection of the curves when extrapolating the intensity ratio I_{338}/I_{334} at low and high concentration regions.

2. Characterizations of Compounds

2.1 Characterizations of Dendrimers

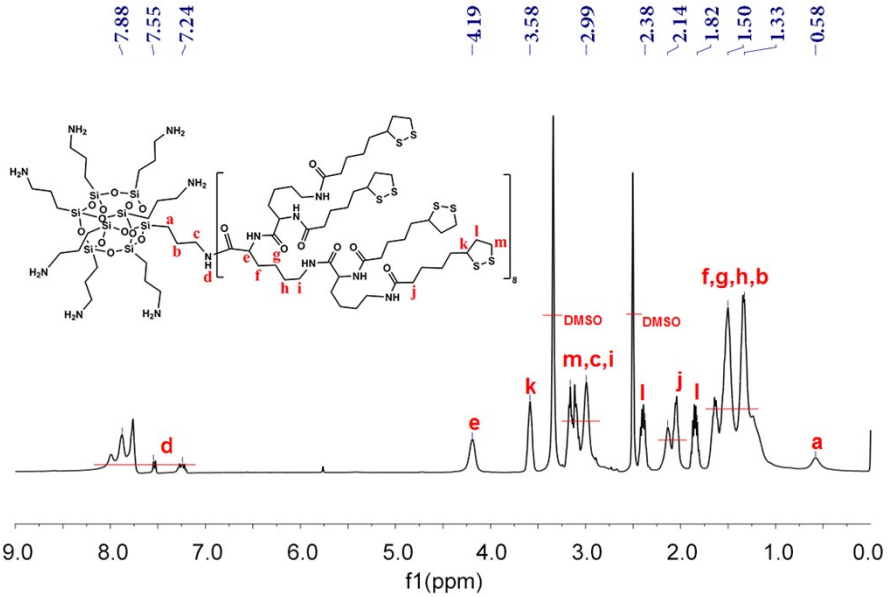

Fig. S1. ^{1}H NMR spectrum of G2-LA$_{32}$ in DMSO-d_6 (400 MHz).

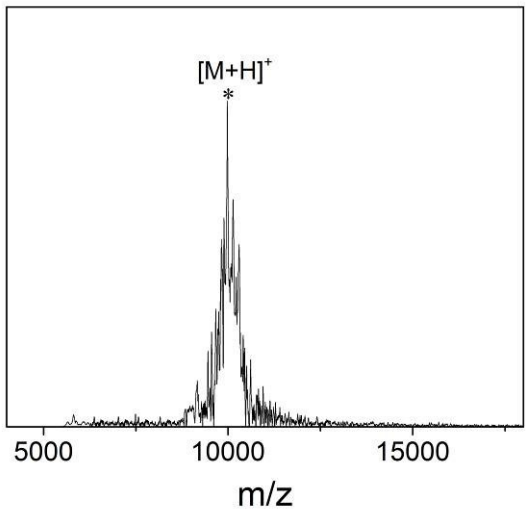

Fig. S2. MALDI-TOF mass spectrum of G2-LA$_{32}$ (m/z, [M+H]$^{+}$): 9977.64 (calculated), 9977.67 (observed).

2.2 Characterizations of mPEG-LA

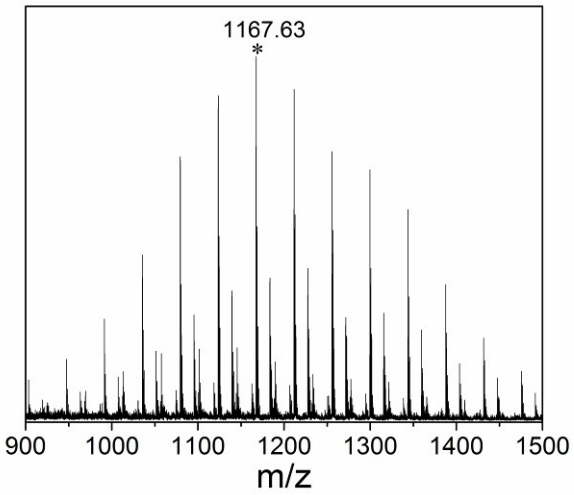

Fig. S3. MALDI-TOF mass spectrum of mPEG-LA (m/z, $[M+H]^+$): 1167.63 (calculated), 1167.63 (observed). $[M+Na]^+ = 264.09 + 44.03\ n + 22.99$ ($n > 0$) (observed).

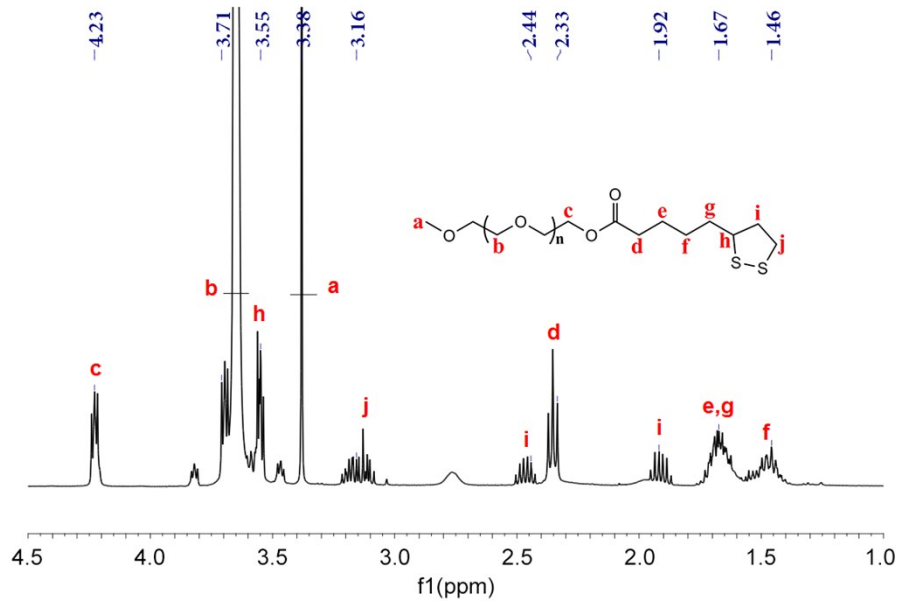

Fig. S4. ^1H NMR spectrum of mPEG-LA in $CDCl_3$ (400 MHz).

3. Results

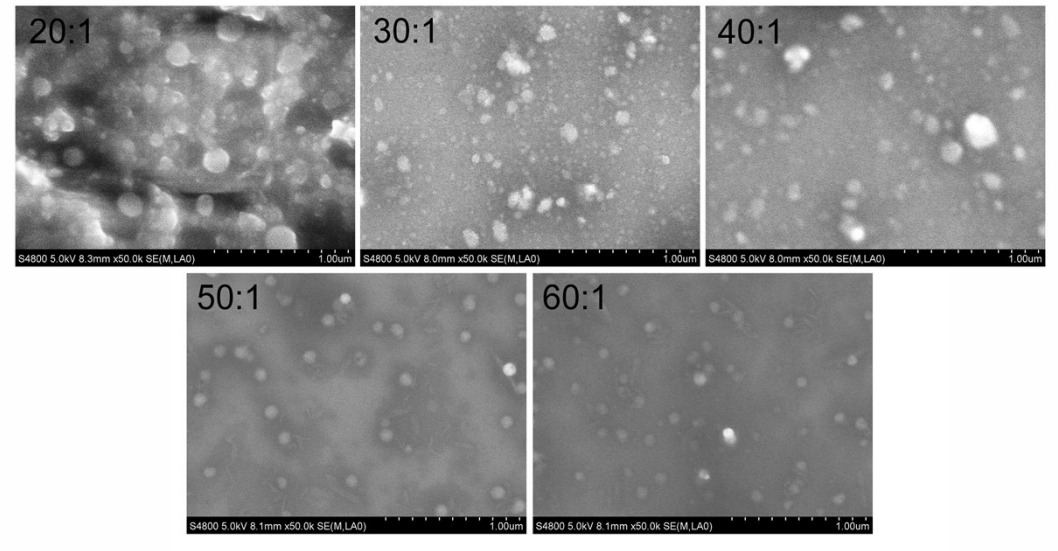

Fig. S5. SEM images of TDNs with different molar feed ratios from 20:1 to 60:1 (mPEG-LA/G2-LA_{32}).

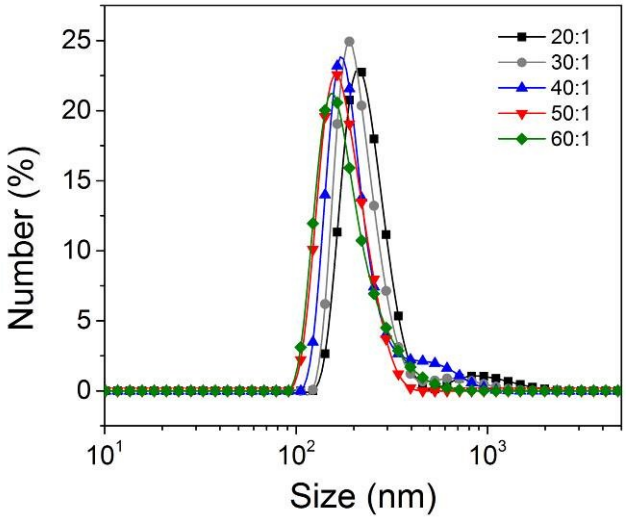

Fig. S6. Size distributions of TDNs with different molar feed ratios from 20:1 to 60:1 (mPEG-LA/G2-LA_{32}).

Table S1. The DLS results of TDNs with different molar feed ratios from 20:1 to 60:1 (mPEG-LA/G2-LA_{32}).

Molar Ratio	Size (nm)	Diffusion Coefficient (μ^2/s)	PDI
20:1	298.3 ± 20.79	0.865 ± 0.060	0.506 ± 0.106
30:1	246.7 ± 13.93	1.17 ± 0.006	0.455 ± 0.057
40:1	213.9 ± 22.06	1.59 ± 0.042	0.249 ± 0.016
50:1	174.3 ± 15.48	1.87 ± 0.015	0.179 ± 0.028
60:1	176.2 ± 10.06	1.89 ± 0.026	0.213 ± 0.090

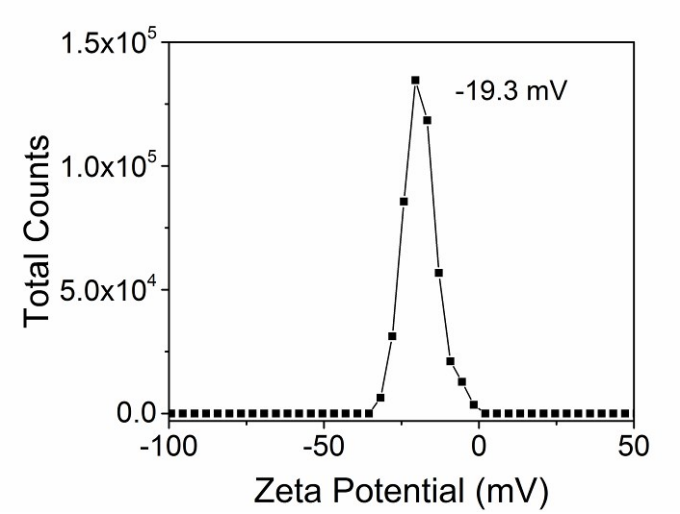

Fig. S7. Zeta potential of TDNs in aqueous solution with a concentration of 100 μg/mL.

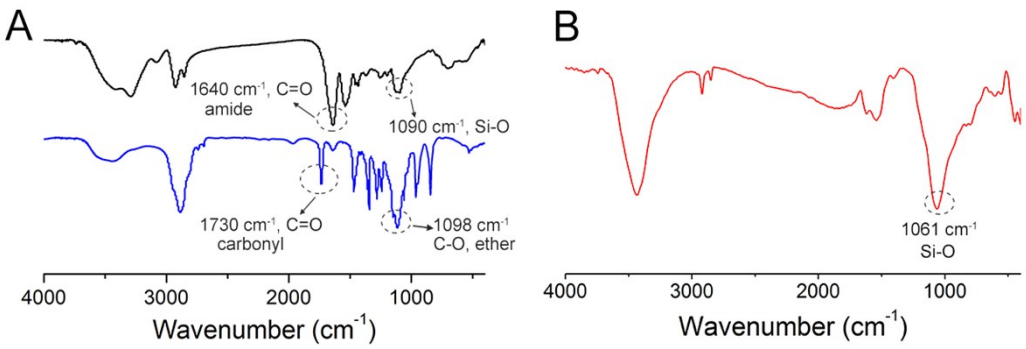

Fig. S8. (A) FT-IR spectra of mPEG-LA (Blue line) and G2-LA_{32} (Black line). (B) FT-IR spectrum of G2-LA_{32} after heating to 900 ℃.

The composition ratio of mPEG-LA and G2-LA_{32} in TDNs was calculated according to the equations:

$$w_a \cdot x + w_b \cdot y = z \quad (1)$$

$$w_a + w_b = 100\ \% \quad (2)$$

where, w_a is the mass percent of mPEG-LA in TDNs, w_b is mass percent of G2-LA_{32} in TDNs, and x, y, z are the residue mass of mPEG-LA, G2-LA_{32}, TDNs, respectively.

After heating to 900 ℃, the residue of mPEG-LA, G2-LA_{32} and TDNs are 0.37%, 2.39% and 12.52%, respectively. Thus, according to eq (1) and eq (2), the mass percent of mPEG-LA in TDNs is 83.37% and the mass percent of G2-LA_{32} in TDNs is 16.63%.

The average molecular weight of mPEG-LA is 1188.32 g/mol, and the molecular weight of G2-LA_{32} is 9976.64 g/mol. The mole (n) is determined by mass (m) and molecular weight (M)

$$n = m/M \quad (3)$$

Thus, the mole ratio of mPEG-LA to G2-LA_{32} in TDNs is determined as 42.09.

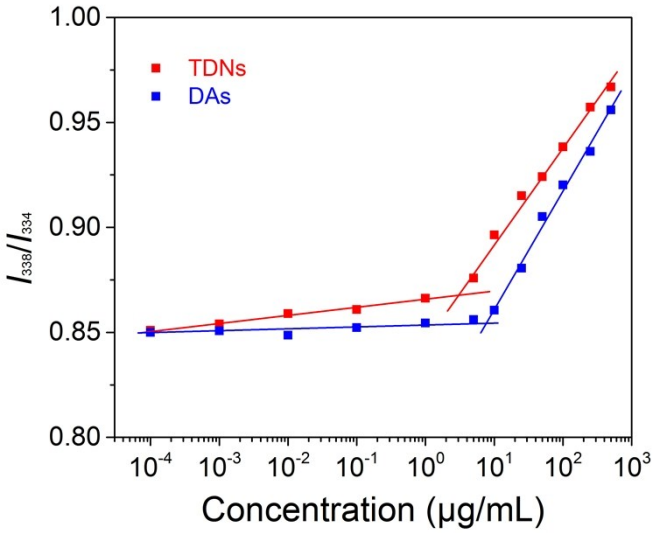

Fig. S9. I_{338}/I_{334} plotted as a function of concentration of DAs and TDNs. [Pyrene] = 6.7×10^{-7} M. The critical micelle concentrations of DAs and TDNs were determined to be 7.73 and 2.52 μg/mL^{-}, respectively.

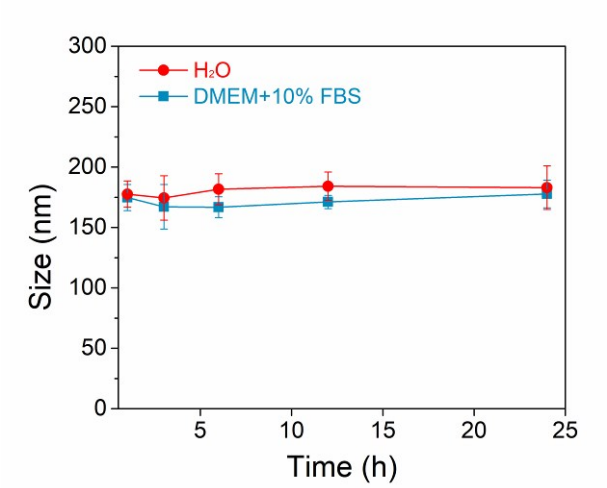

Fig. S10. Average size changes of TDNs as a function of time in DMEM+10% FBS.

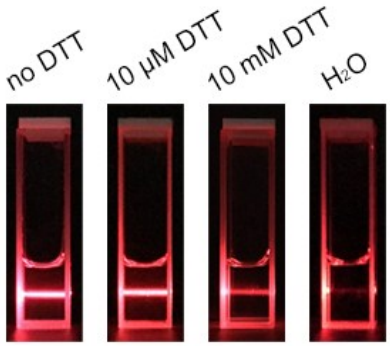

Fig. S11. The Tyndall effect of TNDs after treated with DTT (0, 10 μM or 10 mM) for 12 h. The pure water was used as control.

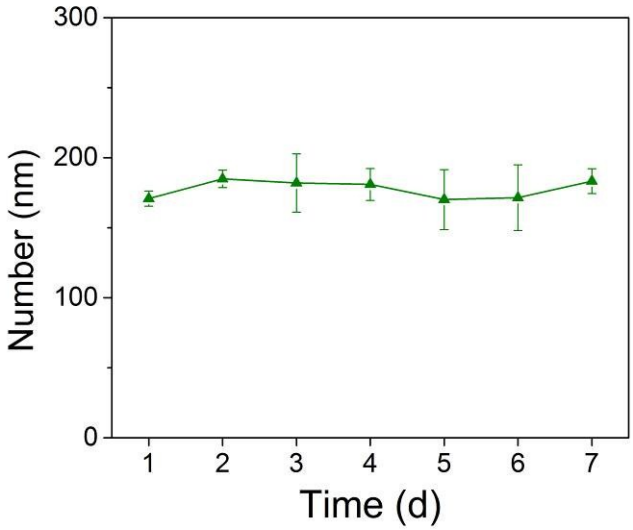

Fig. S12. Size changes of TDNs in the presence of 10 μM GSH as a function of time.

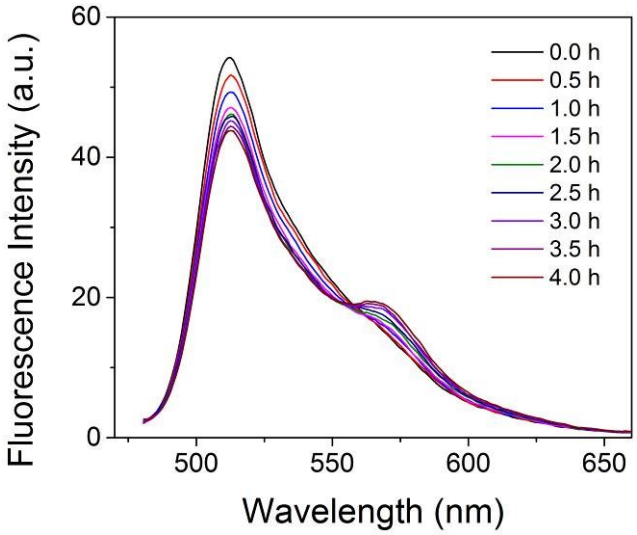

Fig. S13. Fluorescence spectra of the mixed solutions of TDNs prepared with 1 wt% DiO/DiI tracing the development of FRET between the dyes over time in the presence of 10 μM GSH.

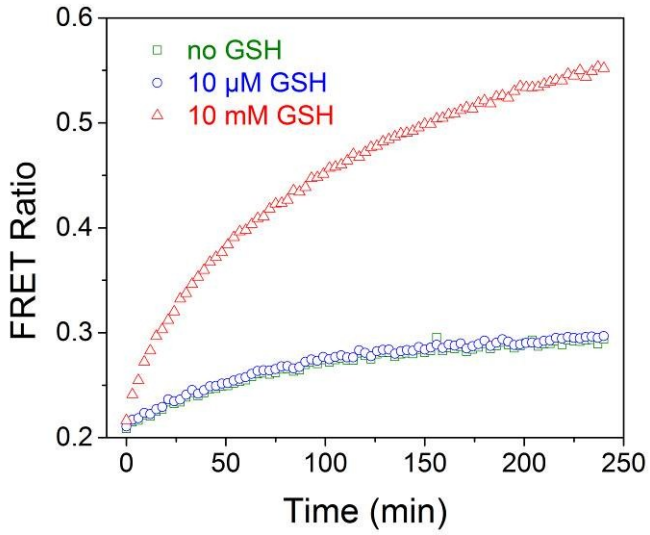

Fig. S14. FRET ratio *vs* time plot of the mixed solutions of TDNs (100 μg/mL) in different concentrations of GSH.

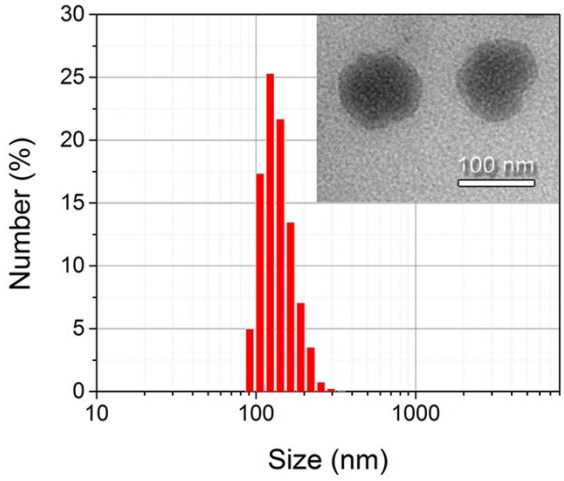

Fig. S15. DLS result and TEM image (the insert) of D-TDNs (100 μg/mL).

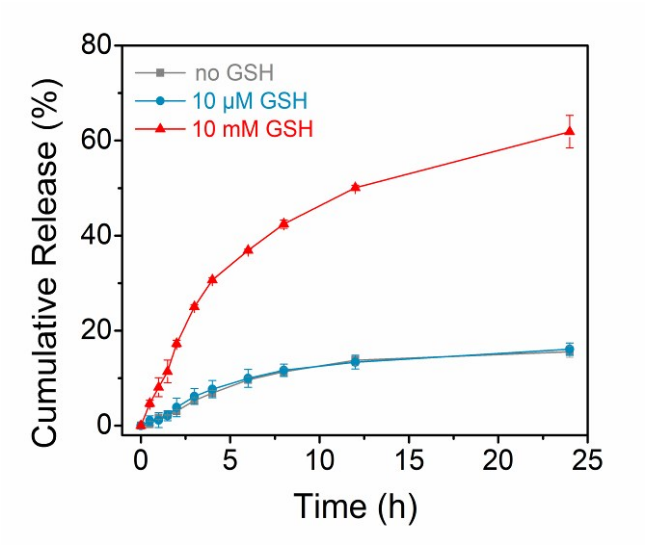

Fig. S16. *In vitro* release profiles of DOX from D-TDNs under different concentration of GSH at 37 ℃ and pH 7.4.

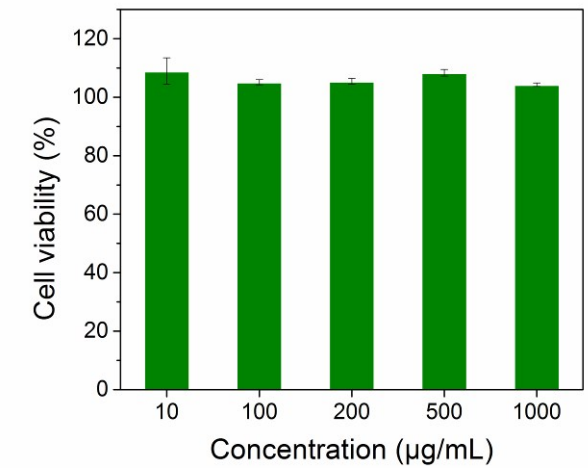

Fig. S17. Cell viability of 3T3 cells incubated with TNDs for 48 h. Data are presented with mean ± standard deviation (n = 5).

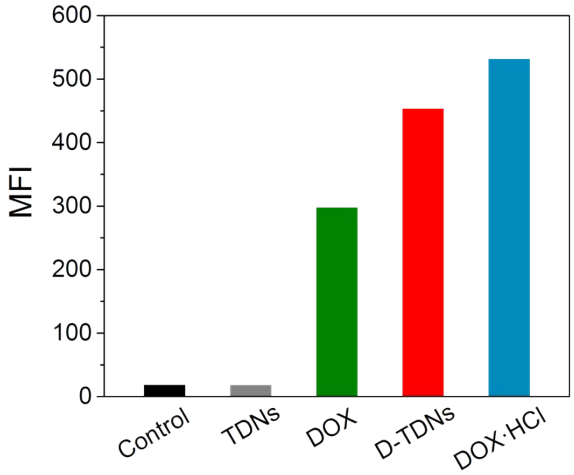

Fig. S18. Mean fluorescence intensity of 4T1 cells after treated with TDNs (100 μg/mL), DOX (10 μg/mL), DOX·HCl (10 μg/mL) and D-TDNs (100 μg/mL, 10 % drug loading) for 3 h.

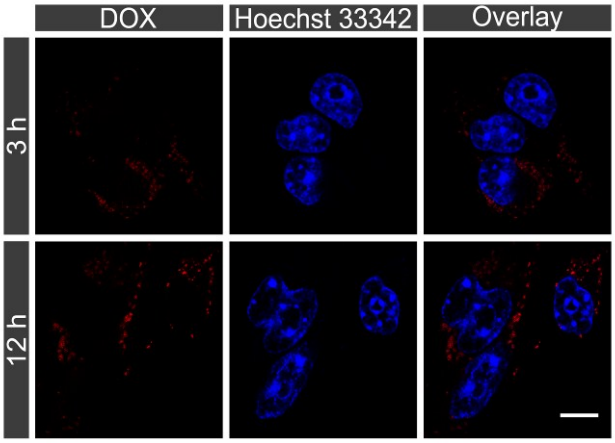

Fig. S19. Intracellular distribution of DOX (2 μg/mL) in 4T1 cells. Cell nuclei were stained with Hoechst 33342 (blue). Scale bar: 10 μm.

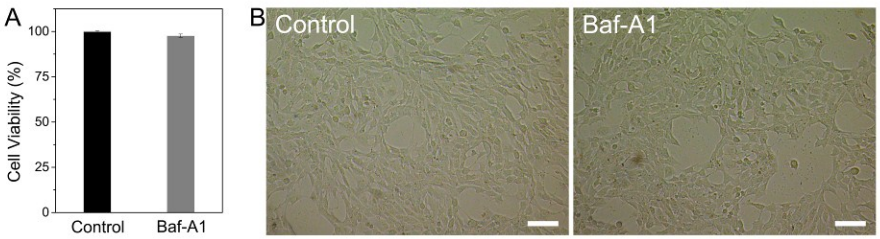

Fig. S20. (A) Cell viability of 4T1 cells incubated with Baf-A1 for 1 h and further incubation for 48 h. (B) Relative cell images after treating with Baf-A1 for 1 h. Scale bar: 100 μm.

As compared with the blank control, the cells pre-treated with Baf-A1 (1.0 μM) for 1 h showed no difference on cell morphology, and the cell viability was more than 95%, suggesting that Baf-A1 has non-cytotoxicity on 4T1 cells.

Table S2. Pharmacokinetic parameters of DOX·HCl and D-TDNs after intravenous administration at an equivalent dose of 5.0 mg DOX/kg mouse body weight (n = 3 per group).

Parameter	DOX·HCl	D-TDNs
$MRT_{0-\infty}$ [a] (h)	0.494	27.713
$t_{1/2z}$ [b] (h)	0.832	19.781
$AUC_{0-\infty}$ [c] (μg/mL×h)	59.536	719.15

[a] Mean retention time.

[b] Elimination half-life.

[c] Area under curve.

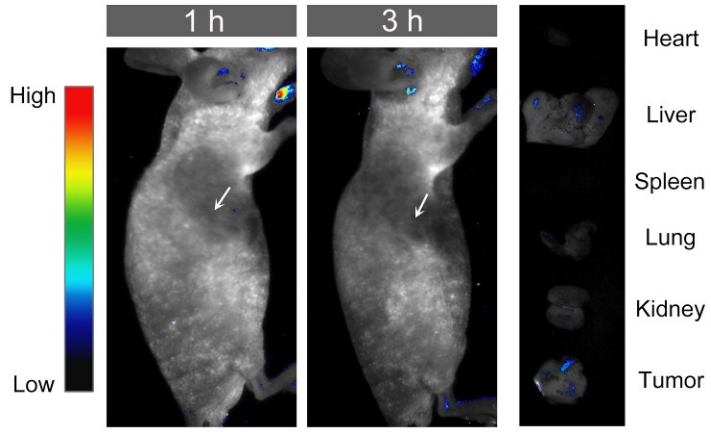

Fig. S21. *In vivo* imaging of nude mice bearing 4T1 tumor and ex vivo image of major organs (heart, liver, spleen, lung and kidney) and tumor tissues at 6 h post-injection of saline.

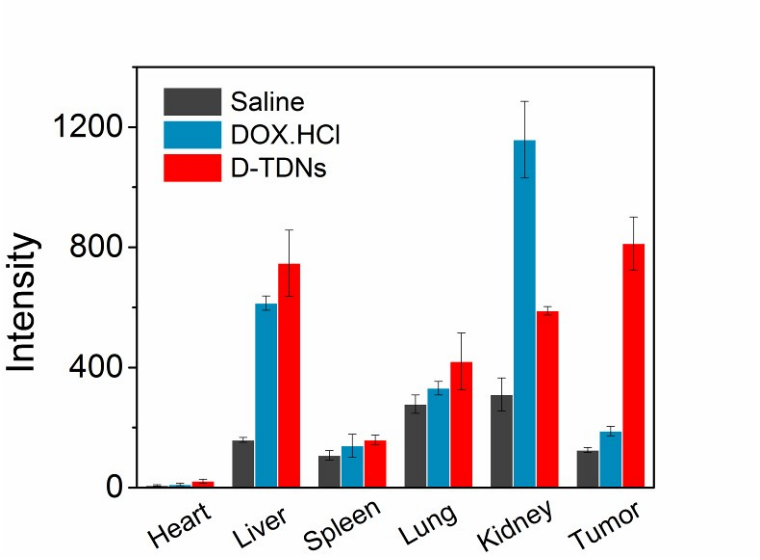

Fig. S22. Quantification of DOX distribution of tumor and major organs (heart, liver, spleen, lung and kidney) by a Maestro *in vivo* imaging system. Tumor were excised 6 h after intravenous injection of DOX·HCl and D-TDNs.

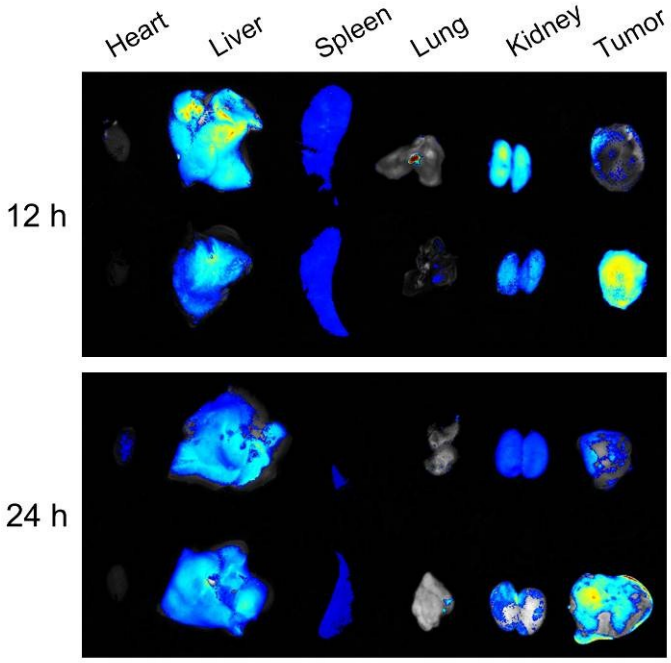

Fig. S23. *Ex vivo* fluorescence imaging of tumors and organs (heart, liver, spleen, lung and kidney) after 12 h or 24 h intravenous injection of DOX·HCl, D-TDNs (5 mg DOX/kg)

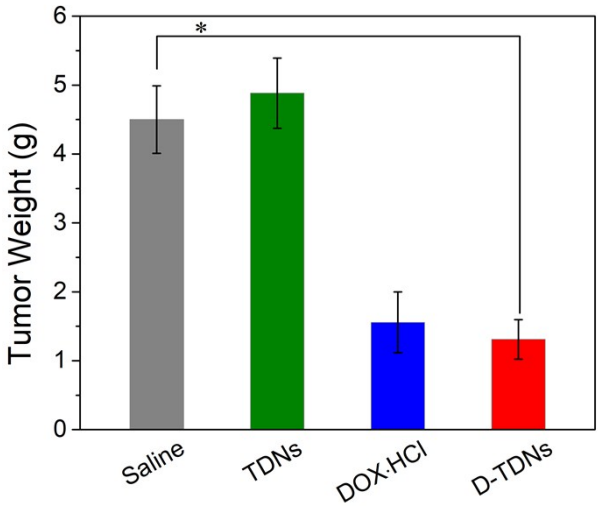

Fig. S24. Tumor weight of 4T1 tumor-bearing mice administrated with saline, TDNs, DOX·HCl and D-TDNs for 18 d (5 mg DOX/kg, $n = 6$, $^{*}p < 0.05$).

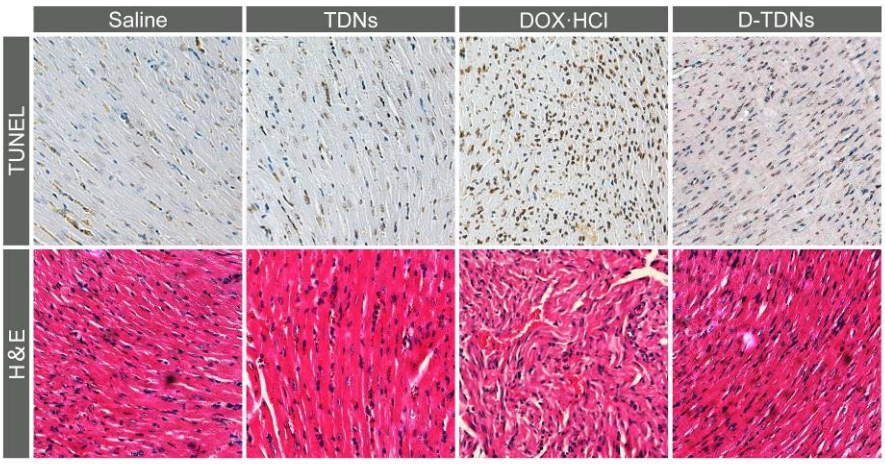

Fig. S25. Histological examination of heart (×200) separated from mice injected intravenously with saline, TDNs, DOX·HCl, D-TDNs at day 18 after first injection.

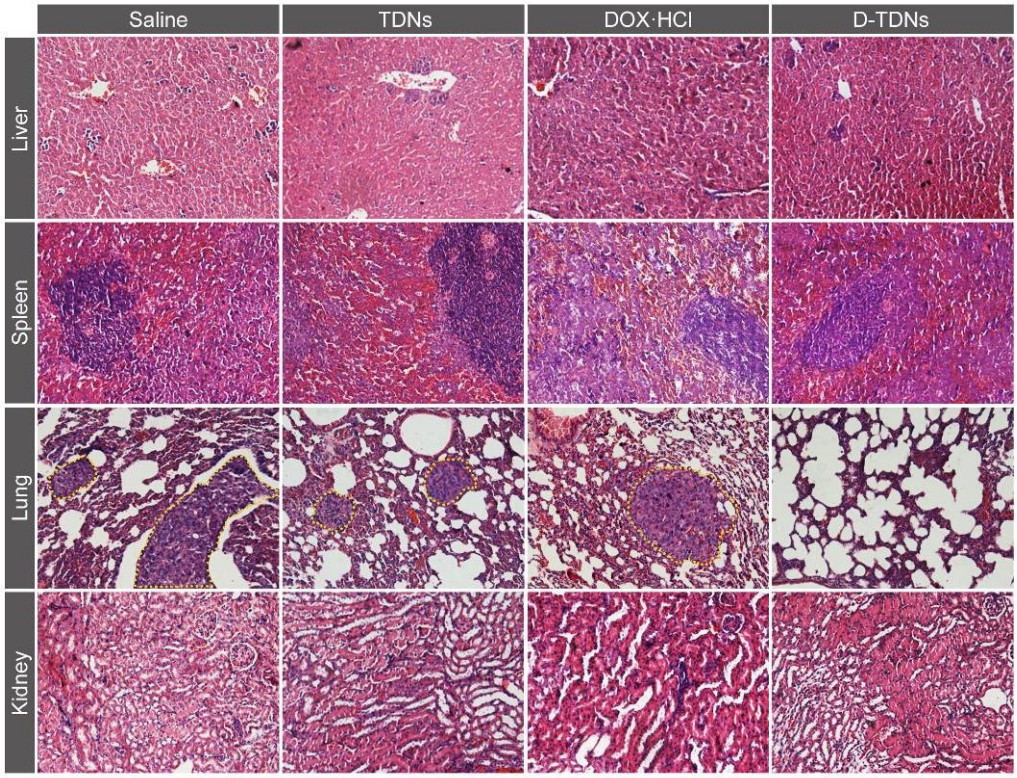

Fig. S26. Histological examination of major organs (×100) separated from mice administration with saline, TDNs, DOX·HCl and D-TDNs at day 18 after first injection.

Histologic examination showed that the organs (liver, spleen, lung, kidney) of mice administrated saline and TDNs were normal, without obvious histopathological abnormalities, degenerations or lesions, indicating no cells and tissues damage. Furthermore, distinct pulmonary metastasis, which was marked by yellow line, was shown in the lung slice of saline administered group. In contrast, few metastasis sites

were observed in the lung of the D-TDNs group, even better than the DOX·HCl group. Thus, it could be concluded that D-TDNs offered the satisfactory therapeutic effects as well as reduced side effects.